

## Small satellite REIMEI for auroral observations<sup>☆</sup>

Hirobumi Saito<sup>a,\*</sup>, Masafumi Hirahara<sup>b</sup>, Takahide Mizuno<sup>a</sup>, Seisuke Fukuda<sup>a</sup>, Yousuke Fukushima<sup>a</sup>, Kazushi Asamura<sup>a</sup>, Hiroyuki Nagamatsu<sup>a</sup>, Koji Tanaka<sup>a</sup>, Yoshitsugu Sone<sup>a</sup>, Nobukatsu Okuizumi<sup>a</sup>, Makoto Mita<sup>a</sup>, Masatoshi Uno<sup>a</sup>, Yoshimitsu Yanagawa<sup>a</sup>, Takuya Takahara<sup>a</sup>, Ryosuke Kaneda<sup>a</sup>, Takashi Honma<sup>a</sup>, Takeshi Sakanoi<sup>c</sup>, Akira Miura<sup>a</sup>, Toshinori Ikenaga<sup>a</sup>, Keita Ogawa<sup>d</sup>, Yasunari Masumoto<sup>a</sup>

<sup>a</sup> Japan Aerospace Exploration Agency (JAXA), Institute of Space and Astronautical Science (ISAS), Japan

<sup>b</sup> Tokyo University, Japan

<sup>c</sup> Tohoku University, Japan

<sup>d</sup> Advanced Engineering Services Co. Ltd.

### ARTICLE INFO

#### Article history:

Received 2 February 2011

Received in revised form

25 April 2011

Accepted 9 May 2011

#### Keywords:

Small satellite

Aurora observation

Advanced technology demonstration

Small instruments

### ABSTRACT

This paper describes the outline and the five years' on-orbit results of the small scientific satellite REIMEI for aurora observations and demonstrations of advanced small satellite technologies. REIMEI is a small satellite with 72 kg mass, and is provided with three-axis attitude control capabilities for aurora observations. REIMEI was launched into a nearly sun synchronous polar orbit on Aug. 23rd, 2005, from Baikonur, Kazakhstan, by Dnepr rocket. REIMEI satellite has been satisfactorily working on the orbit for five years at present as of January, 2011. Three-axis control is achieved with accuracy of  $0.1^\circ$  ( $3\sigma$ ). Multi-spectrum images of aurora are taken with 8 Hz rate and 2 km spatial resolution to investigate the aurora physics. REIMEI is performing the simultaneous observation of aurora images and particle measurements. REIMEI indicates that even a small satellite launched as a piggy-back can successfully perform unique scientific mission purposes.

© 2011 Elsevier Ltd. All rights reserved.

## 1. Introduction

The Institute of Space and Astronautical Science, Japan Exploration Agency (ISAS/JAXA), have launched a series of scientific satellites, including planetary spacecraft as well as astronomical observation satellites. Although the missions have achieved fruitful scientific results, these satellites cost nearly \$200 million and take longer than seven years to be developed. The launch frequency of the scientific satellites decreases significantly in this decay.

In addition to these “big, expensive, slow” missions, the authors planned to launch “small, inexpensive, fast” piggy-back satellites as good tools to demonstrate new technologies

and perform science observations. The piggy-back satellite REIMEI (INDEX: Innovative Technology Demonstration Experiment) has been developed since 2002 and launched in 2005 [1,2]. REIMEI has been still functioning for five years at present as of January, 2011. This paper describes the outline of the on-orbit results of REIMEI.

## 2. Outline of mission and satellite description

### 2.1. Aurora observation

Auroral phenomena in the polar regions of the Earth, the Jupiter, etc., are characterized by auroral emissions of a wide wavelength range, energy, and pitch-angle distributions of electrons and ions. A main scientific purpose of REIMEI is an investigation on small-scale dynamics of terrestrial auroras, namely, their spatial distributions and time variations, and their correspondence to spectrum

<sup>☆</sup> This paper was presented during the 61st IAC in Prague.

\* Corresponding author. Tel.: +815033622657;

fax: +81427598368.

E-mail address: [saito.hirobumi@jaxa.jp](mailto:saito.hirobumi@jaxa.jp) (H. Saito).

properties and spatial distributions of charged particles, which generate the auroral emissions [1]. One of observation instruments is a multi (three)-channel auroral camera (MAC) using three CCD imagers, and another is electron and ion energy spectrum analyzers (ESA/ISA) with top-hat type electrostatic optics.

The most advanced approach in the auroral observation by REIMEI is the simultaneous measurement of auroral emissions and particles using the satellite attitude control and the satellite orbit. Fig. 1 explains details of the observation. The simultaneous measurement provides us with  $64 \times 64$ -binning pixel two-dimensional auroral images covering about  $70 \times 70 \text{ km}^2$  area at 110-km altitude for three wavelengths of 428, 558, and 670 nm every 120 ms, and energy-pitch angle distribution functions of auroral particles with energies of 12 eV–12 keV for electrons and 10 eV/q–12 keV/q for ions every 20 ms.

The attitude of REIMEI is controlled so that the field-of-view of MAC covers the REIMEI footprint that is the projection point of REIMEI at altitude of 110 km (aurora region) along a magnetic field line. This means that the ESA/ISA could measure auroral particle properties on the same geomagnetic field line on which the auroral emissions could be observed by MAC.

2.2. Advanced small satellite technologies

The engineering mission is to demonstrate the advanced small satellite technologies on orbit. The advanced technologies to be tested in REIMEI satellite are as follows: (i) three-axis attitude control system with  $0.1^\circ$  pointing accuracy in 70 kg satellite [3,4], (ii) integrated satellite-control based on high-speed 32 bit RISC processor (SH-3, 60MIPS, triple voting system) [1,5], (iii) lithium ion rechargeable battery with laminate package as main battery system [6], (iv) solar-concentrator paddle with thin film reflectors and high efficiency (27%) solar cells [7,8], (v) variable emittance radiator with material of perovskite [9], (vi) Miniature GPS receiver modified based upon automobile navigation GPS receivers [10–12].

2.3. Satellite description

REIMEI is a small scientific satellite with size of  $72 \times 62 \times 62(\text{H}) \text{ cm}^3$  and mass of 72 kg [1,2]. REIMEI has

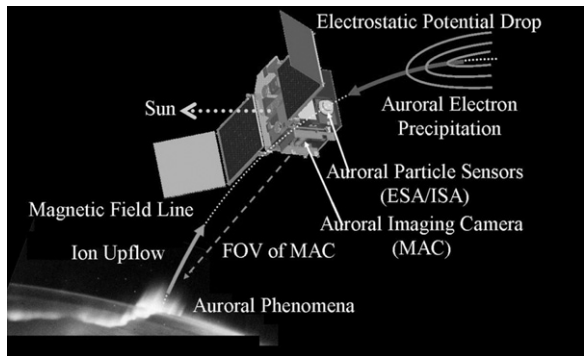


Fig. 1. Configuration of simultaneous auroral observations with REIMEI.

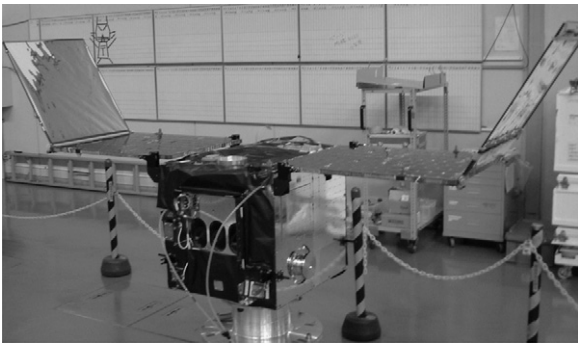


Fig. 2. REIMEI Satellite with solar paddles deployed.

Table 1  
Main specifications of REIMEI.

Item	
Mission	Observation of aurora (Imagers and particle analyzers) 7 Technologies demonstration
Mass	72 kg (Bus 61 kg, Payload 11 kg)
Size	$72 \times 62 \times 62 \text{ cm}^3$
Orbit	Nearly sun synchronous $608 \times 655 \text{ km}$ , Noon Time
Launch	Dnepr Rocket, 2005/8/23
Life	Has been working 65 months @ 11/01
Power	150 W, Solar-concentrated with Thin Film Reflector, 3-Junction Cell, 3.0 AH $\times$ 2 Lithium ion battery 3-Sequential partial shunt
Attitude	Bias-momentum three-axis stabilization Pointing error: $0.05\text{--}0.1^\circ$ Determination error: $0.05^\circ$ Attitude stability: $0.004^\circ/\text{s}$ $1 \times \text{RW}(0.5 \text{ Nms})$ , $3 \times \text{MTQ}(6 \text{ Am}^2)$
Communications	S-Band USB Uplink bit rate: 1 kbps Downlink bit rate: 132/64/32/16/8 kbps

two solar-concentrated deployable solar paddles with power capability of 150 W. Fig. 2 is a photograph of REIMEI with solar paddles deployed. Table 1 describes the main specifications of REIMEI.

REIMEI satellite was designed based on an integrated computer system [5]. Almost all tasks for the satellite control are executed on the integrated control unit (ICU). For the processor on the onboard computer board (OBC) of the ICU, the commercial RISC CPU, Hitachi SH-3 (SH7708, 60 MIPS) is employed. Since the SH-3 is not radiation-hardened, three processors with DRAMs and EEPROMs compose a triple voting system in order to ensure fault-tolerance. If a voter error occurred due to a single event upset (SEU), the wrong cell is automatically reconfigured by copying DRAMs and register data of a SH-3 from a different cell. It takes about two seconds to execute the reconfiguration process.

A system block diagram of the satellite is shown in Fig. 3. The ICU is directly connected with almost all instruments, including sensors (STar Tracker, Spin/Non-spin-type Sun Aspect Sensor, Geomagnetic Aspect Sensor, and Fiber Optical Gyroscopes) and actuators (Reaction Wheel and Magnetic TorQuers) for attitude control,

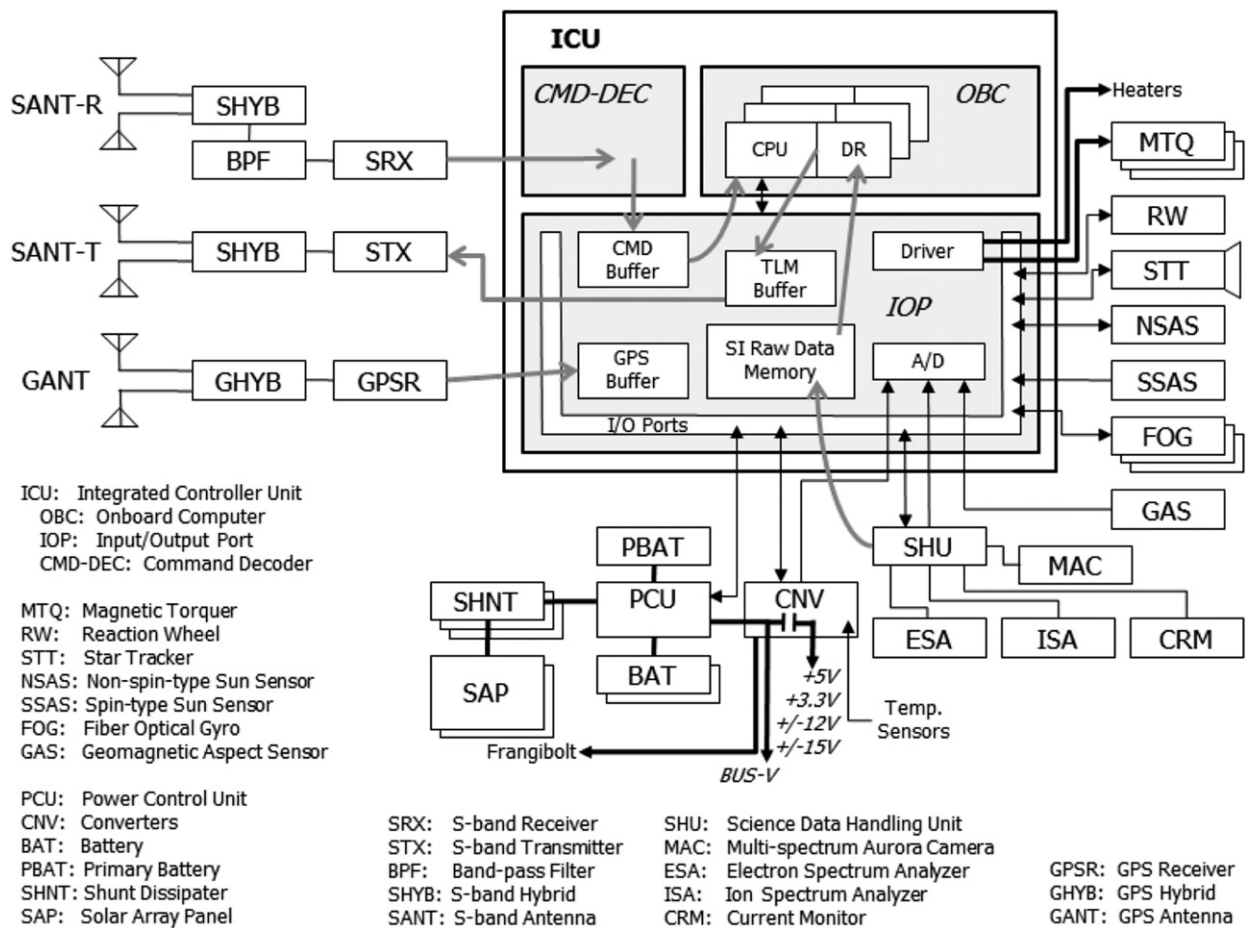


Fig. 3. System block diagram of REIMEI.

an S-band receiver (SRX), a transmitter (STX), etc., in a star-like fashion. In other words, the ICU takes a combined role of a data-handling unit, attitude control electronics, and heater control electronics in conventional satellite design. For the sake of system compactness, there is no data bus outside of the ICU and all the instruments are controlled directly in the address space of the processor. Input/output ports (IOP) for the peripheral components are developed with space-qualified anti-fuse FPGAs.

Software modules corresponding to each task are executed in a cyclic manner according to 8 Hz external interruptions: Attitude control and determination, command reception and distribution, telemetry formatting and down-link control, collection of house-keeping data, and some mission modules (i.e., aurora observations and GPS). The whole software is designed and implemented in-house.

The attitude control system of REIMEI is a bias-momentum three-axis stabilized system [3,4]. The detail of the attitude control is described in Section 4.

The command link is S band communication with 1 kbps, and the telemetry link is S band with 131, 64, 32, 16, and 8 kbps. The main control station of REIMEI is newly developed Sagami-hara small satellite station with a 3 m antenna [5].

The cost of REIMEI is about 4 million US dollars without JAXA personal expenses. The total cost of REIMEI is about 6.5 million US dollars in which JAXA personal expenses are included. REIMEI satellite was designed, developed, and tested by JAXA in-house team. There was not a main contractor company in REIMEI satellite. Common instruments such as batteries, solar paddles were fabricated by the satellite manufacturing companies. The data handling instruments and power management instruments were fabricated by small venture companies. Many young staff and students were involved in the REIMEI development, working together with the venture companies. These development activities are very effective to activate space developments and space education.

#### 2.4. Optimization for scientific mission

REIMEI has two purposes, namely the scientific purpose and the engineering purpose for a small satellite. At satellite design and development, however, we paid special care to optimize the scientific mission. Scientists joined in REIMEI project team and discussed intensively with the engineers to optimize the satellite for the scientific purposes.

The most interactive subsystem with the science mission is the attitude control subsystem, which was designed to meet the observation requirement such as the attitude control mode, the pointing accuracy, the pointing stability, and the accuracy of attitude determination. REIMEI performs the measurement of magnetic field and energy spectrum of particles. Therefore satellite was kept thoroughly clean against magnetic field. Especially the magnetic line tracking mode for the particle measurement is dedicatedly designed so that the magnetic torquers are powered off for about five minutes without generating any magnetic disturbance.

REIMEI is operated mainly by the aurora scientists who are not necessarily familiar with satellite technologies. Therefore REIMEI and its ground station are designed and instrumented so that even an inadequate operation does not lead REIMEI to a fatal condition. We describe in Section 7.2 its robust system with fault detection, isolation, and recovery function.

The fact that the scientists still continue to operate REIMEI for five years after launch shows that REIMEI satisfies their sciences.

### 2.5. Development and launch

The concept study of REIMEI started in 1998 in order to activate small satellite researches and to promote capability building of young staff. In 1999 the aurora observation was selected as a scientific mission by the science steering committee of ISAS. The engineering and science team started incubation of noble ideas on the small satellite. The proto model of the data processing instrument, the power control unit, and the satellite structure had been developed in 2000–2002. The project spent hard time to obtain the budget of the satellite. Finally the flight model (FM) was developed in 2003 and then the first FM test was conducted in 2004. In the summer of 2004, it was suddenly decided that REIMEI would be launched in the summer of 2005 as a piggy-back with JAXA OICETS satellite by Dnepr rocket from Baikonur. In 2005, the environmental test and the final FM test were conducted. Then in the middle of July, 2005 REIMEI was shipped to Baikonur through Moscow. The project members were at the launch site to conduct the final check prior to the launch.

INDEX was launched by a Dnepr rocket from the Baikonur Cosmodrome Launch site in the Republic of Kazakhstan in 2005 on Aug. 23, 21:09:58.8 UTC. REIMEI is injected into a nearly sun-synchronous orbit with the local time of about 12:00, which is adequate for aurora observations. Apogee and perigee heights were 654.866 and 608.731 km, respectively. The sun acquisition was performed by three magnetic torquers. Libration dumping control was the first stage of the initial startup sequence, and was finished for 1.9 h as scheduled. In the second stage, spin-up control was started. A nominal spin rate of 1.0 rpm was achieved. Then sun acquisition was activated and the sun angle reached 60° for 5.6 h from separation. At this point, the satellite automatically deployed the solar array paddle (SAP) and stayed at the safety state.

INDEX first passed over Japanese ground stations after 6 h from launch. The main ground station for the launch

phase (Uchinoura 20 m diameter antenna) received the telemetry signal on Aug. 24, 3:10 UTC, which filled us with great joy.

## 3. Small onboard instruments

Developments of small on-board instruments with new ideas and technologies are required in order to implement high satellite performances in limited mass, volume, and power of a small satellite. This section describes the outlines and the five years' on-orbit results of the small instruments.

### 3.1. Miniature GPS receivers

In these days tiny GPS receivers have been applied to auto-mobile navigation system and mobile instruments. These GPS receivers have mass of about 10 g and power consumption of less than 1 W.

A miniature space GPS receiver has been developed for REIMEI based on the automobile-navigation receiver (Japan Radio Corporation, CCA-370 HJ) [10,11]. Fig. 4 shows a photograph of CCA-370HJ receiver. It is an eight-channel receiver with frequency (L1) with code ranging. We expanded the frequency sweep range up to  $\pm 57$  kHz in order to cover the large Doppler shift ( $\pm 45$  kHz) on orbit. We tested the performance for low earth satellite applications by means of a GPS simulator. The range error caused by the receiver was estimated to be 0.9 m in RMS by the GPS simulator. The receiver can tolerate 20 krad of radiation and is SEL-free for 200 MeV protons.

The modified GPS receiver in REIMEI works perfectly on orbit. Cold start positioning has been confirmed repeatedly to finish within 25 min from start. We performed orbit determinations with GPS position data for 60 s and evaluated the residual position error between the orbit determination and the GPS position data. The short term random error of GPS positioning is as large as 1.5 m for a PDOP (position dilution of positioning) of 2.7 on-orbit, which is as good as on ground.

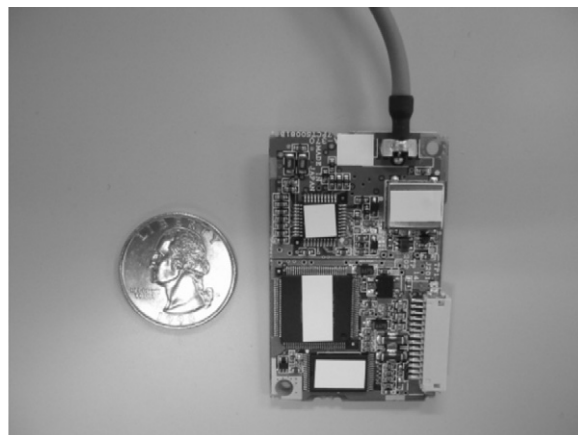
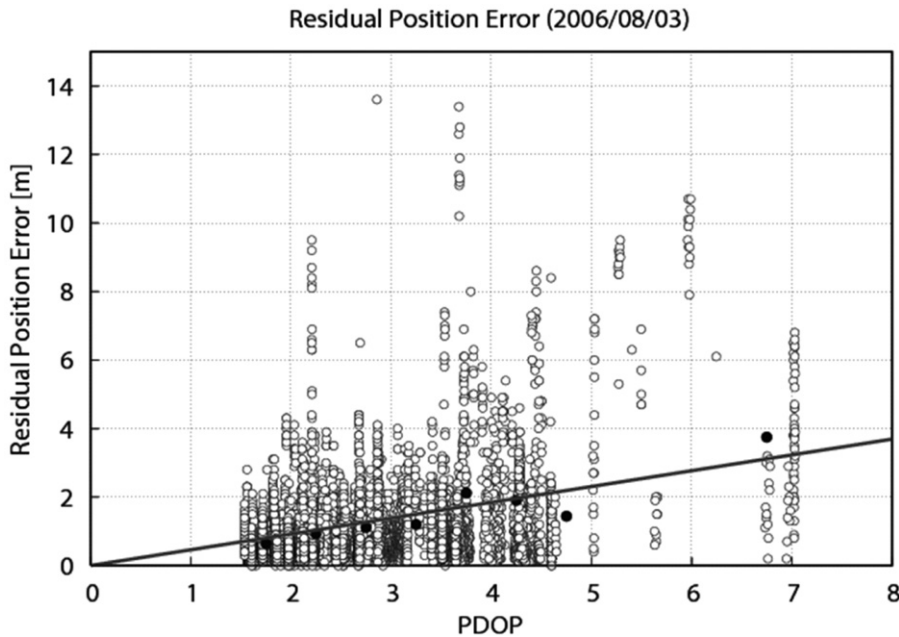


Fig. 4. Photograph of miniature space GPS receiver modified from automobile navigation.





**Fig. 5.** Relation between residual position errors and position dilution-of-positioning (PDOP) values based upon GPS on-orbit data. Solid circles are RMS values for each bin of PDOP value. Straight line is least-square-error fit of solid circles.

Fig. 5 shows the relation between PDOP values and residual position errors. The PDOP axis is divided into nine bins and the RMS value of the residual position errors in each bin is indicated in Fig. 5 by solid circles. As expected, the RMS values of residual position errors are nearly proportional to the PDOP values. The straight line in Fig. 5 is the least-square-error fit of the solid circles and its slope is 0.46 m, which corresponds to the standard deviation of range error due to the receiver.

This miniature GPS receiver has been perfectly working for five years. Especially it is very user-friendly that it starts position measurement automatically in less than 25 min once powered-on. This miniature space GPS receiver is now on market [12] as a promising receiver with low cost and medium performance.

### 3.2. Solar-concentrator paddle

#### 3.2.1. Merit of thin film reflector

For the solar-concentrator paddles on REIMEI, the two paddles without reflectors weigh 2.6 kg and generate about 120 W of power. The specific power of the solar paddles without the reflectors is 46 W/kg. The structure of the solar-concentrator paddles is shown in Fig. 6. There are two wings that have thin film reflectors. The reflective wings have a total mass of 0.32 kg and enhance solar intensity by a factor of 1.25. The power increase due to the reflectors is about 30 W. The specific power of the solar-concentrator paddles is 51 W/kg. The specific power of the reflectors, which is defined as the ratio of the power increment and the reflector mass, is 94 W/kg. In REIMEI, a single reflector is attached to the end of a solar paddle in order to use a single-stage deployment mechanism. If a double-stage deployment was applied to the system, two

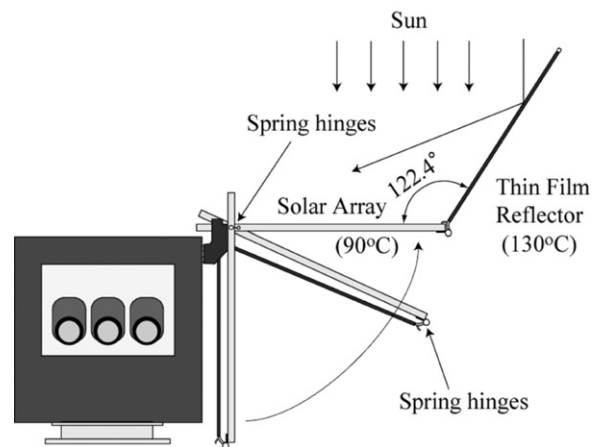


**Fig. 6.** Structure of solar paddles and reflectors.

reflectors could be attached at both side facets of the paddle, doubling the effect of solar concentration.

#### 3.2.2. Avoidance of power degradation

The Boeing BSS-702 Satellite Bus launched in around 2000–2001 had been equipped with double-sided solar-concentrator paddles with thin film reflectors [13]. However, they suffered from power loss beyond the prediction, which was nearly a linear drop in power as a function of time. It has been reported that the root cause of the power loss is contamination coupled with UV/radiation exposure and shrinkage. It is predicted for BSS-702 that the maximum temperature of the solar cell is around 120 °C while the concentrator film is around 95 °C. This temperature condition may induce contamination on

the concentrator film. Outgas from the cell panel may condense on the reflector surface, which is at a lower temperature. It has been qualitatively confirmed that UV and radiation exposure causes loss of surface reflectance of the pre-contaminated surface and also causes the concentrators to shrink. To avoid the power degradation observed in the BSS-702 satellite, special care was devoted to the design and manufacturing of the REIMEI solar concentrator. One modification to the reflector structure was to ensure that the deployment angle would be independent of the shape of reflector film. The other modification was that the thermal design of the thin film reflector was improved to prevent possible contamination.

For REIMEI, the maximum temperature of the cell panel was estimated to be 90 °C under 1.3 solar illumination with the reflector. The solar cells are triple junction InGaP/GaAs/Ge cells with 27% efficiency, which is very effective in reducing the cell temperature even for a solar concentration ratio of 1.3. To avoid possible contamination of the reflector, the temperature of the reflector should be higher than the cell temperature of 90 °C. Thin film polyimide (25  $\mu$ m) aluminized on the both sides (UTC-025 S-AANN manufactured by Ube Industries, Ltd.) was selected as a reflector. The aluminized back side has low IR emittance, which is effective in keeping the film temperature high. The solar absorptance and IR emittance were measured to be 0.08–0.09 and 0.01–0.02, respectively. Consequently, the temperature of the reflector was estimated to be 130 °C in the sunshine given an incident angle of 60°, which corresponds to a sun angle of 0° with respect to the Z-axis of the satellite body. During eclipse, the temperature was estimated to be –70 °C. Flight data shows a cell temperature of 90 °C in the sunshine with 1.3 solar concentration and –60 °C during eclipse. The assessment of possible power degradation was performed by the Office National d'Etudes et Recherches Aerospatiales (ONERA/DESP) in France. Their result indicates that, due to the higher temperature of the reflector and the relatively low temperature of the cell, the predicted degradation due to contamination is very small for REIMEI; less than 1% per year.

### 3.2.3. Performance on orbit

The performance of the solar-concentrator has been evaluated on orbit. At a constant bus voltage, the solar current at the moment, when the shunt current is zero, should be proportional to the solar intensity on the solar paddle. Fig. 7 shows the solar current at the moment of zero shunt current as a function of the sun angle. If there were no the solar-concentrators at the solar paddle of REIMEI, the solar current would have a cosine dependence on the sun angle as shown by the broken line in Fig. 7. The real line in Fig. 7 shows the predicted value for the real case with the solar-concentrator. We find that the solar-concentration effect is enhanced in the sun-angle range between –15° and 15°. The solid squares indicate the measured solar current on orbit as a function of sun angle. The solar concentration vanishes at sun angles greater than 25° due to the reflection geometry. The predicted solar concentration at a sun angle of 0° was 1.25. The measured values (solid squares) are in good coincidence with the predicted values.

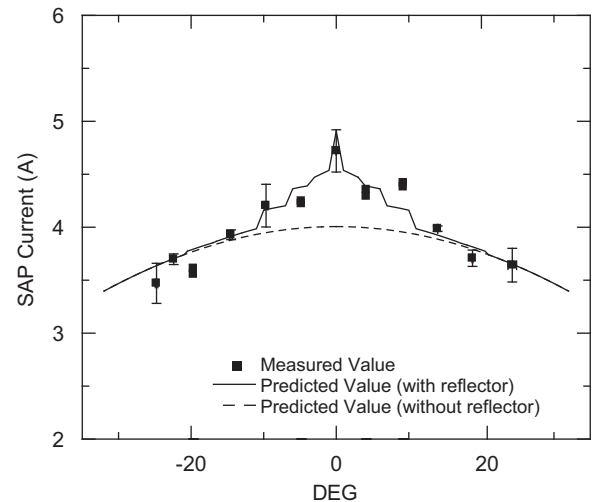


Fig. 7. Solar current as function of solar angle. Real line and broken line are predicted values with and without solar-concentrator, respectively. Solid squares ■ indicate measured values on orbit.

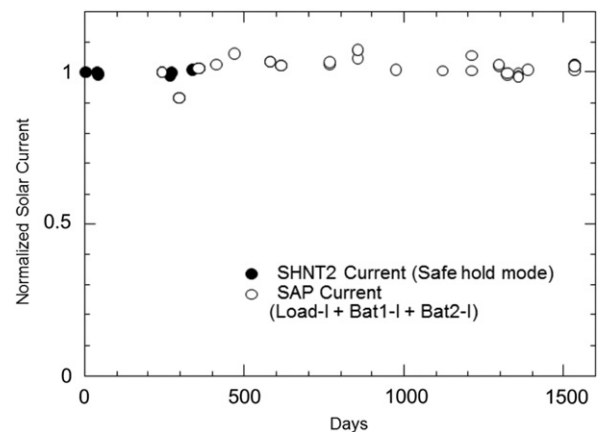


Fig. 8. Five years' on-orbit trend of solar current with solar-concentrator paddles. Sun angle is 0°.

In order to verify our improvement in concentrator design, we monitored the trends in power generation for REIMEI at a sun angle of 0° since launch. Fig. 8 shows the five years' trend of measured solar current at a sun angle of 0°. The values are normalized by the initial values just after the launch. Solid circles are shunt currents for a safe hold mode, which depend linearly on the solar current. The open circles are the sums of the bus load current and the battery charge currents, which are equal to the solar current. It is observed that there is no degradation of the solar current or solar power. At present, we can conclude that our counter measures against contamination-induced degradation are effective.

### 3.3. Laminate lithium-ion battery

Laminate package batteries are light weight and safe for over pressure. Recently laminate package is applied to medium capacity batteries of several AH.



Fig. 9. Photograph of laminate package cell of lithium-ion battery.

Lithium-ion secondary batteries based on laminate package cells were applied to REIMEI [6]. The rated capacity of the cell is 3.0 AH. Fig. 9 is a photograph of the laminate package cell of a lithium-ion battery. The laminate package cells are potted with resin and reinforced by the aluminum housing to enhance the tolerance against vacuum environment in space. Seven cells are connected in series to realize a 28 V-class bus battery. The energy density of the battery is about 70 WH/kg.

When aurora observation is performed on orbit above the South Pole, 0.78 A discharge current was first applied for 25 min. It was followed by 0.96 A discharge for 5 min and then 1.63 A discharge for 3 min. The ground tests have proceeded ahead to on-orbit operations to predict the operability of REIMEI on orbit. In the case of the ground test 1.0 A constant discharge current is applied to the cell for 35 min at 25 °C.

Orbital performance of the battery is calibrated based on difference of the discharge rate between the ground test and the flight operation. The difference results in the different voltage drop by the DC impedance of the battery cells. Fig. 10 shows the trend of end-of-discharge voltage (EODV) for the ground test and for the five years' on-orbit data after calibration.

The batteries in REIMEI experience about 5400 charge–discharge cycles in a year. EODVs drop every 5400 cycles in the season when the aurora observations are executed at the end of eclipse above the South Pole. Until 10,000 cycles (2 years after launch) a good agreement between the ground test and the on-orbit data is found in Fig. 10. However, the cells at the ground indicate a gradual decrease of EODV after 15,000 cycles (3 years after launch) as a symptom of degradation while EODVs of the batteries on orbit remain almost constant even at 25,000 (5 years after launch). The batteries on orbit are thermally controlled around 20 °C, while the cells at the ground test are thermally controlled at 25 °C as a worst condition for the batteries. In general, a lower temperature makes life of a battery longer. The lower temperature by 5 °C may result in the almost constant EODV for five years on orbit.

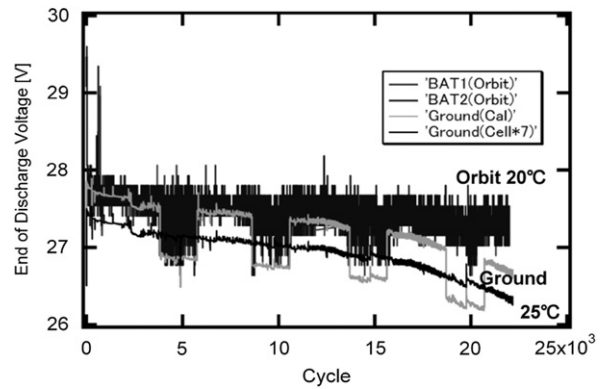


Fig. 10. Five years' trend of end-of-discharge voltage (EODV) for REIMEI on-orbit operation (20 °C) and ground simulation results (25 °C) after calibration. Data of a single cell is multiplied by series number of batteries (7) so as being compared with battery voltages.

#### 4. Fine three-axis control with magnetic torquers

One typical observation of aurora phenomena is a simultaneous observation of particle and image. E/ISA analyzes the energy spectra at REIMEI, and MAC captures an auroral image at the footprint of the magnetic field line, where aurora emission is excited by the particle which E/ISA observes. Such an observation requires satellite with three-axis stabilization and inertial pointing capability. We developed the optimized attitude control system with the limited resource [3,4].

##### 4.1. Attitude control instruments

The sensors for attitude control are a spin type sun sensor (SSAS), a two-dimensional sun sensor (NSAS, accuracy 0.05°), a star tracker (STT, accuracy 1 arcmin) at the X panel, a three-axis geomagnetic field aspect sensor (GAS), and three-axis fiber-optical gyroscopes (FOG). Temperature of FOG is controlled within 0.2 °C to achieve relatively high bias-stability of 0.1°/h, although that of the specification is 3°/h. The field of view of the aurora camera MAC is in the X direction. The attitude determination algorithm is based upon the extended Kalman filter, which estimates the bias rates of FOGs and the attitude of REIMEI.

The actuators of the attitude control are a small reaction wheel (RW, 0.5 Nms) in the Z direction, and three-axis magnetic torquers (MTQ, 6 Am<sup>2</sup>).

The reaction wheel provides agility as well as control around the Z axis, and MTQs generate attitude control torque around the X and Y axes. In this point, magnetic torque control plays an important role.

An onboard instrument that has certainly a life time is the reaction wheel. We have carefully monitored the conditions of the reaction wheel. Fig. 11 shows a trend of the friction torque of the ball bearings at the nominal rotational speed 2000 rpm for five years on orbit. Also Fig. 11 shows the bearing temperature and the –Z panel temperature on which the reaction wheel is fixed.

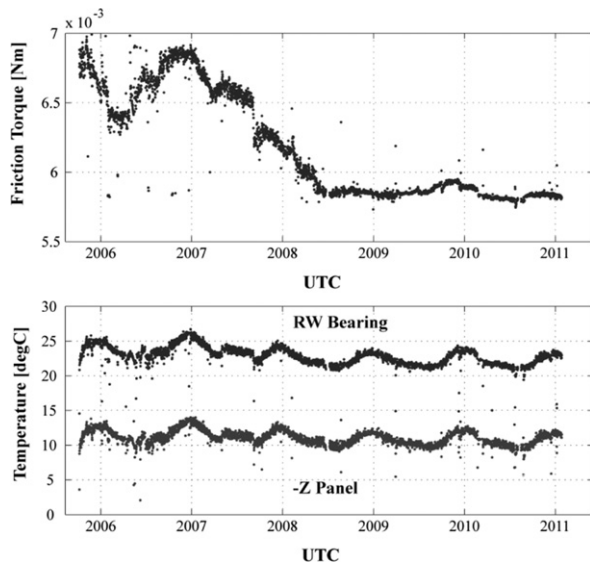


**Fig. 11.** Five years' trend of friction torque (upper graph), and temperatures (lower graph) of bearing in reaction wheel and of  $-Z$  panel on which reaction wheel is fixed.

The friction torque is calculated by a disturbance observer in the attitude control onboard software by means of input torque to the motor and torque for change of the wheel rotational speed. The friction torque seemed to have a positive temperature-dependence in 2005–2006. In 2007–2008 the friction torque decreased from 6.8 to 5.8 mN-m. Since the middle of 2008 the friction torque remains stable around 5.8 mN-m and there is no symptom of degradation. One of possible explanations for these phenomena is as follows: at the manufacturing phase lubricant may be excess, resulting in a positive-temperature dependence of the friction torque. Excess lubricant seems to leak and the amount of lubricant reach to an adequate amount in 2007–2008, which decreases in the friction torque. This monitoring method may be an adequate one for health monitoring of the reaction wheel.

#### 4.2. Magnetic torque control

The issue on the magnetic torque control is to find the magnetic moment  $\mathbf{M}$ , which generates the required torque on two axes ( $X$  and  $Y$ ) in a geomagnetic field  $\mathbf{B}$ . The cross-product law and the method with pseudoinverse matrix are widely applied. However,  $B_z=0$  is a singular point in these methods.

The MTQs are saturated at this singular point and generate a large disturbance torque on  $Z$  axis. To improve this behavior, a novel algorithm [4] is proposed in the REIMEI project. The new algorithm is based on singularity robust inverse (SR-inverse) method. The SR-inverse is proposed in the field of robotics, and also frequently used in a torque steering law of control moment gyros (CMG). The orbit performance of REIMEI reveals that the SR-inverse method is very effective to reduce disturbance torque near singular points of  $B_z=0$ .

Generally, the dominant attitude disturbance source for LEO small satellites is a residual magnetic moment. Other disturbance sources, such as a gravity gradient, a solar radiation pressure, and air drag, have relatively small effects for small satellites. One approach to suppress disturbance is to enhance the feedback controller. This is an orthodox way. It, however, depends on several conditions such as the sensor noise, the computational performance and the plant model accuracy.

Another approach is a feed-forward cancellation of the residual magnetic moment. In this case, performance depends on the accuracy of residual magnetic moment estimation. To estimate it with on-orbit attitude data, a residual magnetic moment observer is applied to REIMEI satellite. The estimated disturbance torque, which is the output of disturbance observer, is calculated on the ground. The period of disturbance torque is found to be about a half of the orbital period. With this estimated disturbance torques and the measured geomagnetic field  $\mathbf{B}$ , the residual magnetic moment  $\mathbf{M}_r$  is estimated, with least square method, to be  $\mathbf{M}_r=[0.51, 0.042, 0.11] \text{ Am}^2$ . This estimated  $\mathbf{M}_r$  is uploaded to spacecraft via command. This value is used to REIMEI as a feed-forward value, to cancel the residual magnetic moment.

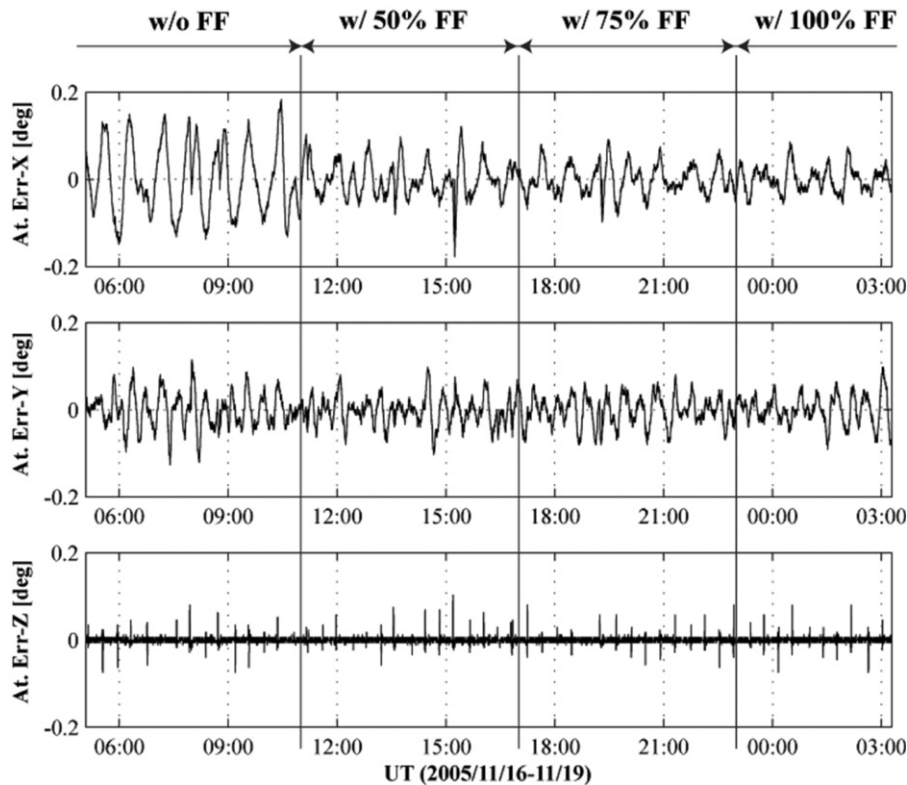
#### 4.3. Performance on orbit

Fig. 12 shows the effect of feed-forward cancellation. The upper, middle, and lower graphs are the attitude-control angle errors of the  $X$ ,  $Y$ , and  $Z$  axes, respectively. Each graph consists of four time periods. In the first, labeled “w/o FF,” attitude was controlled by only the feedback controller, without any feed-forward cancellation. In the second, labeled “w/50% FF,” feed-forward cancellation was applied, but with only 50% of the estimated value. In the third, the value for feed-forward cancellation was increased to 75% of  $\mathbf{M}_r$ . Finally, in the fourth period, 100% feed-forward cancellation was applied. These gradual steps clearly show the effect of  $\mathbf{M}_r$  feed-forward cancellation. It indicates the validity of the proposed  $\mathbf{M}_r$  estimation and the cancellation method. The on-orbit attitude control error is about  $\pm 0.2^\circ$  with no feed-forward cancellation. With full  $\mathbf{M}_r$  feed-forward cancellation, the pointing error decreased 25%, to less than  $\pm 0.05^\circ$ .

Just before the launch, measurement of residual magnetic moment  $\mathbf{M}_r$  was carried out in a magnetic shielding chamber for REIMEI in the final flight configuration. It was concluded that the residual magnetic moment of the REIMEI is  $\mathbf{M}_r=[-0.054, -0.039, -0.069] \text{ Am}^2$ . The attitude error was as large as  $\pm 0.2^\circ$ , when this measured value was applied for feed-forward cancellation. The estimated value on the orbit was much more effective than the measured one on the ground. It suggests that the residual magnetic moment was varied after the ground measurement. The reason, however, is still a mystery.

During one month, July 2006, REIMEI carried out about 90 aurora imaging observations. These observations indicate that worst-of-worst feedback error is about  $0.1^\circ$ . The attitude determination error has been evaluated to be less than  $0.05^\circ$ , therefore RSS pointing accuracy is estimated to be  $0.1^\circ$ . Total pointing accuracy is also





**Fig. 12.** Attitude control errors of X, Y, and Z axes as functions of time. Feed-forward cancellation of  $\mathbf{M}_r$  (residual magnetic moment) is added with various intensity to conventional feedback control. “w/ 50% FF” means that 50% of output from feed-forward control law is added to feedback controller. Feed-forward cancellation with 100% intensity is applied in normal aurora observations and achieves control accuracy of  $0.05^\circ$  ( $1\sigma$ ).

**Table 2**  
Requirement and achievement of REIMEI attitude control system.

	Requirement	Achievement
Absolute pointing error [deg.]	0.5	0.05–0.1
Determination error [deg.]	0.06	0.05
Feedback error [deg.]	0.05	
Attitude stability [deg./s]	0.03	0.004

confirmed with data of aurora imager, and the end-to-end absolute pointing accuracy was revealed to be  $0.05\text{--}0.1^\circ$ , typically. These evaluations clearly indicate that the achieved performance meets the mission requirements, as shown in Table 2.

## 5. Auroral observation

REIMEI has three types of instruments for the scientific purpose to investigate fine-scale structures, dynamics of auroral emissions, and particles. The first is the multi-spectral monochromatic auroral imaging camera (MAC) [14], the second is the set of auroral particle (electron and ion) energy spectrum analyzers (ESA/ISA) [15], and the third is the plasma current probes (CRM). Here, we focus on results using the auroral images and particle spectrograms. The geomagnetic field data is also available due to the measurements by a three-axis geomagnetic field aspect

sensor (GAS). The previous paper [16] presented more detailed specifications of these scientific instruments.

The biggest advance in the auroral observation by REIMEI is the simultaneous measurement of auroral emissions and particles using the precise satellite attitude control and the appropriate satellite orbit. This mode is called Mode-S, mainly characterizing the novel observation method by the REIMEI science payloads for obtaining the fine auroral properties. MAC has the  $1024 \times 1024$  pixels for three wavelength bands. The Mode-S provides us with  $64 \times 64$ -binning pixel two-dimensional auroral images covering about  $70 \times 70 \text{ km}^2$  area at the 110-km altitude for three wavelengths of 428, 558, and 670 nm every 120 ms and energy-pitch angle distribution functions of auroral particles with the energies of 12 eV–12 keV for electrons and 10 eV/q–12 keV/q for ions every 20 ms. The three-axis satellite attitude control is executed so that the field of view of the auroral camera MAC catches the projected footprint of REIMEI position along the local magnetic field line to a 110 km altitude, which is precalculated based upon the orbit information. This means that the ESA/ISA could measure auroral particle properties on the same geomagnetic field line on which the auroral emissions could be observed by MAC. This sequential observation procedure is planned by our science team on the ground before the actual observation and is executed by stored commands transmitted to REIMEI.

The first example of the Mode-S observational results is shown in Fig. 13. This event on August 1, 2007 is valuable for the discussion on the auroral emission-particle correlation in the mid-night auroral region at the REIMEI altitude (about 640 km). In the energy-time spectrogram of precipitating electrons (the bottom of three similar panels), a clear structure of the accelerated electrons is observed after 21:52:16 UT. In this case the maximum energy of electrons was about 2 keV. It is remarkable after 21:52:16 UT that the energy of accelerated electrons drastically varies in the range from a few tens of eV to a few keV. The comparison with the auroral images presented in the lower panels of Fig. 13 is crucial to identify the relation of the precipitating electrons with the aurora emissions. It is clearly recognized that the footprint of REIMEI was crossing a large auroral band. It should also be noted that REIMEI footprint often encountered enhanced blobs of small auroral emissions, all of which are associated with the rapid energy variations of the precipitating auroral electrons. Dotted light red lines connecting the auroral images and the electron energy-time spectrograms are demonstrating these correspondences. These relations of the variations of auroral

forms with the precipitating electrons accelerated by the Alfen waves have been already reported in Refs. [17,18].

The second example, which is not presented here, of the simultaneous observations was the measurements made on February 21, 2006. This type of auroral emergence is called pulsating auroras because the auroral patches repeatedly switch on and off with an almost constant time interval of several seconds. It is observed that the high-energy (more than about 2 keV) electron components are coherently correlated with the periods of the auroral patches emission. Some other particular data analyses have derived an important result that the source/acceleration regions of precipitating electron components causing pulsating auroras are located in the equatorial region of the Earth magnetosphere.

The advanced auroral observations by REIMEI are summarized as follows:

1. REIMEI has successfully been observing the fine-scale properties on auroral emissions and particles through the well planned satellite operation in cooperation with the fine attitude control.

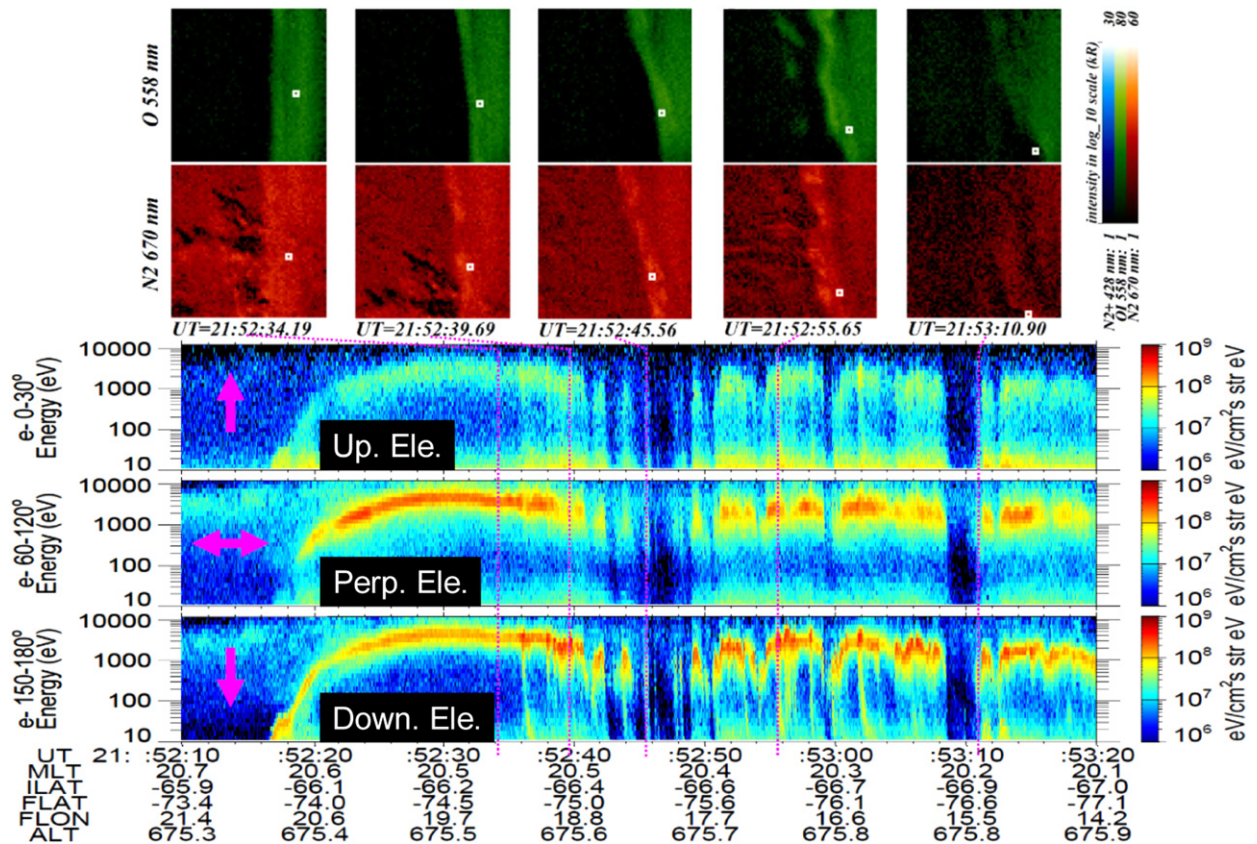


**Fig. 13.** Observational results by ESA and MAC for the event obtained in the southern and nightside auroral region on August 1, 2007. The upper panels with green and red are auroral images at 557.7 and 670 nm, respectively. The emission intensity is displayed by color level, as shown at the righthand of the auroral images. A dot in each image indicates the footprint of REIMEI mapped onto the ionospheric altitude of 110 km along the local geomagnetic field line. The lower three panels show energy (vertical axis) and observational time (horizontal axis) spectrograms for the electrons, which are sorted into three pitch angle ranges (upward: 0–30°, trapped: 60–120°, downward: 150–180°) as depicted by a light red arrow at the leftside in a respective spectrogram. The electron energy flux is displayed by color level, as shown at the righthand of each spectrogram. The observational time of each auroral snapshot image could be referred by the correspondent light red dotted line connecting the image to the spectrograms.

2. The simultaneous observations of auroral emissions and particles show the fine correlation between them in terms of intensities of auroral emission and downward energy fluxes of auroral electrons.
3. Pulsating auroras are often observed by REIMEI and well-correlated with the energy-dispersed precipitating components of electrons.

## 6. Efficient satellite operation

Daily operation of REIMEI is presently performed with the dedicated ground station at ISAS/JAXA Sagami-hara campus [5] using a 3 m diameter antenna on the roof of the main building. If the onboard S-band transmitter (STX) is in the high-power mode, a bit transfer rate of 131 kbps is available with the 3 m antenna. In order to download all the scientific and the engineering data, the Norwegian Svalbard Satellite Station (SvalSat) and the Japanese Showa Base at the South Pole are complementarily utilized. The acquired data is available via FTP without extra cost in a few minutes from loss of sight (LOS) of REIMEI.

The REIMEI operation team consists of young researchers, engineers, and students, who are not necessarily very familiar with all the details of REIMEI functions. Daily satellite operation is performed by one personnel. Most operational software and tools in the ground station were developed by ourselves and a small software house, to allow some autonomy, flexibility and efficiency of operation. Fig. 14 shows the flow of satellite operation item by item.

1,2. Aurora scientists at Tokyo and Sendai, Japan, who plan to observe aurora phenomena with REIMEI, send their command plans for aurora observations to Sagami-hara through internet.

3. They are managed and integrated by CVS (Concurrent Version System) that is a version-management

software system. The merged top-level procedure is very carefully checked as following sequences, since multi-user could send commands conflicted with each other.

4. The automatic generation of a Satellite Operation Procedure (SOP) is a unique system that we have developed to enhance the robustness of satellite operation. The SOP of REIMEI consists of merging “procedure libraries” of individual operation tasks. The procedure libraries, prepared by the people in charge of the individual tasks, are written in XML (eXtensible Markup Language), and are managed with CVS. The XML-based SOP is compiled and automatically generates two files; a human-friendly TeX-style document with XSLT (eXtensible Stylesheet Language Transformation) and an uplink command plan. Some command plans contain programmed command sequences.

5. The generated commands are checked carefully with a prototype model of the ICU before sending them to the real satellite, especially at critical operations. This procedure is used because it is impossible to test all combinations of software tasks running on the integrated computer before launch. We send the command sequences from the ground equipment to the proto model of the ICU for verifications and then simply switch the route of the command to the ground transmitter for satellite operations.

A semi-automatic attitude simulation software tool is utilized as the other command verification tool. It consists of an attitude control software and software that simulate attitude dynamics, space environments, and sensors. This verification is performed at every operation. This tool reads the SOP and automatically generates simulation configuration files. If something suspicious is found in the SOP, the operator is advised how to modify the SOP. When the problem seems to be serious, the tool warns the operator not to use this SOP and to contact the attitude control engineers.

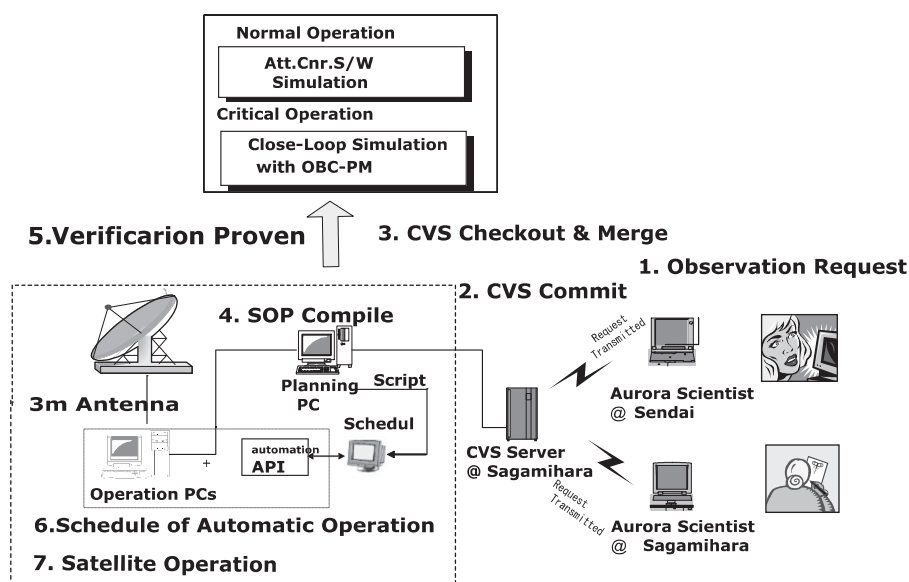


Fig. 14. Flow diagram of REIMEI operation.

6. In conventional system, operators manage sending command, receiving telemetry, antenna driving, satellite health check, emergency action, recording log, etc. by mouse/key board operations. We are in progress to develop a system for automatic REIMEI operation from the ground station. In our new automatic operation, a scheduler software is defined as a substitutive operator. The scheduler reads a schedule file of the operation sequences from SOP. Then, the scheduler manages the satellite operation such as sending command, receiving telemetry, and driving antenna in accordance with an operation time line which was prepared before the operation pass. The scheduler interfaces each PC with the automatic Application Program Interface (API) software, which is equivalent to a mouse/key-board operation. Also, the scheduler performs diagnostics of satellite anomaly based upon the received telemetry data and status of the ground station. In case some anomaly of the satellite is detected, the scheduler initiates an emergency schedule that was prepared depending on the emergency level. If the emergency is serious, the scheduler calls up an appropriate staff for the emergency. This approach is very effective to reduce psychological and physical load of operators. We have a plan to expand the automatic operation to all kinds of satellite operations such as sending stored-commands operations, low-elevation pass operations, etc.

Most of the operation systems could be efficiently constructed with tools for satellite development since the satellite development and the operation are carried out at the same place by the same small group. Many tasks of REIMEI are controlled by the sophisticated integrated-controller ICU. No malfunction due to complexity of ICU occurred in orbit for the five years because of the reliable satellite operation system.

## 7. High reliability with low cost

REIMEI satellite has been working for five years with high reliability. If the ISAS/JAXA personnel expenses are included, the total cost of REIMEI is about 6.5 millions US dollars. The cost of REIMEI is rather low compared to a typical satellite of the same mass class [19]. We describe the effective points to achieve this high reliability with low cost.

### 7.1. Parts policy

The on-orbit failure analysis [20] revealed that most of satellite malfunctions are not random failures that are governed by constant failure rates, but early failures that are caused by inadequate designs or manufacturings. In fact, 41% of satellite malfunctions occur during the first year of operation. Power (48%), data handling and communication (46%) subsystems have a very high ratio of failures during the first year. These subsystems are mostly made of electronic components with high-reliability parts and they should be reliable at least during 3–5 years of operation. High-reliability parts for space, which are endorsed by certification documents, seem not to be cost-effective.

Our parts policy is that we do not use high-reliability parts but rather use cost-effective, reliable parts as follows. We used passive electric parts of Japanese industry-grade, discreet active electric parts of MIL-grade, radiation-tolerant FPGAs, and commercial high-performance LSIs with triple voting or error correction codes. Active devices are confirmed to be tolerant against total ionizing dose of 10–20 krad. Components that contain parts with a risk of single event latch-up are protected by circuit breakers. We carried out intensive ground tests to eliminate initial parts failures and design problems. Circuit electrical boards are designed to enable easy modification and re-work.

### 7.2. Fault detection, isolation, and recovery

A fault detection, isolation, and recovery (FDIR) system is implemented compactly in REIMEI since all data handling is processed in the integrated data system of ICU instrument. The FDIR system is carefully designed and tested on ground based on the 30 years' experiences of Japanese scientific satellites. The other reason of the cost effectiveness is that there is no need to make official documents about details of the satellite system since the team member of satellite development and operation are well overlapped.

REIMEI is daily operated mainly by aurora scientists, who are not necessarily familiar with satellite technologies. The FDIR system of REIMEI is very robust and reliable. There are three levels of the FDIR system. The first one is against a computer fault mainly related to single event upset due to space radiation. The onboard computer (OBC) is a triple voting system with Hitachi SH-3 as described in Section 2.3. The single event upset of the processor is handled by the automatic reconfiguration of the computer in two seconds. The second one is against an attitude anomaly and a software under-voltage control (UVC) detection. The third one is against a software runaway, a fault of the computer hardware and a hardware UVC detection. In the second and the third cases, the satellite switches into a safe-hold, sun-pointing mode. These three levels of the FDIR are as follows:

1. OBC Anomaly. Faults of the onboard computer itself such as a voter error, a two-bit error of DRAMs, and a synchronous error of three processors activate automatically the reconfiguration of the onboard computer based on three processors. As shown in Fig. 15, the actual number of cell reconfigurations observed in orbit has been 19 times in the first two years. The pluses (+) denote the projected ground positions where the reconfiguration process was activated. We can see in Fig. 15 that most of the errors certainly occurred over the polar regions. Additionally the DRAM one-bit errors, which are corrected by the error correcting code, are also plotted in Fig. 15. Since the one-bit errors are detected not only by direct access (circle ○, 28 events) of the user's program but also by memory patrol (triangle △, 7 events) of the error correcting code every 30 min, there is a little



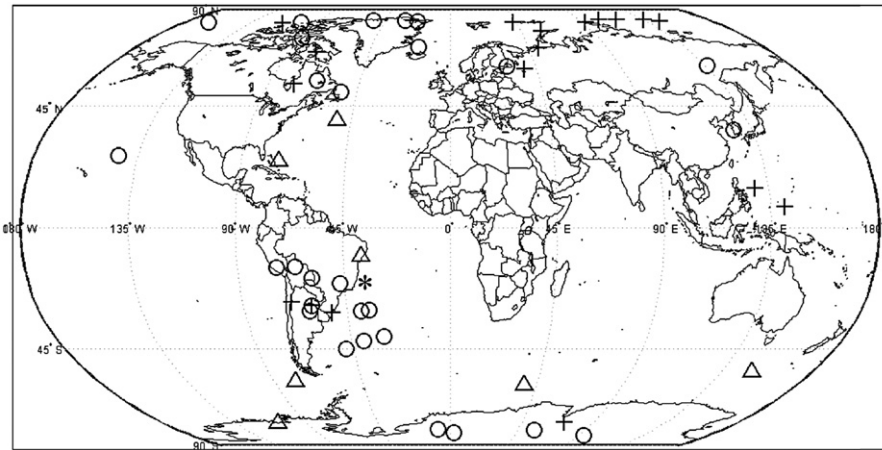


**Fig. 15.** Error map of ICU onboard processor for two years from launch. Pluses (+) denote cell reconfiguration (Total 19 events) due to voter errors (3 events), synchronous errors (2 events), and DRAM 2 bit errors (14 events). Circles (○, 28 events) and triangles (△, 7 events) denote DRAM 1 bit errors detected by direct access and memory patrol at 30 minutes interval, respectively. DRAM 1 bit errors are corrected by error correcting code. \* denotes position of NMI event at June 21, 2006.

ambiguity in the projected ground position. Most of the errors certainly occurred over the polar regions and the south Atlantic anomaly (SAA) region.

2. Attitude Anomaly and Software UVC Detection. REIMEI is a three-axis stabilized satellite with solar wing paddles. If the Z axis is far away from sun direction much more than 30°, the power balance is endangered. We chose a bias-momentum control for sake of satellite safing.

Detection functions of faults related to attitude and electrical power are implemented in the attitude, power, and house-keeping (HK) subsystem. Fault detection items of attitude control subsystem are the sun angle calculated based on the satellite attitude, the eclipse timer, the angular momentum of the reaction wheel, and the total angular momentum of the satellite. Fault detection items of power subsystem are the voltage of two batteries by software, the ampere hour counter through one orbit cycle, and the eclipse timer. Once one of these faults is detected, the satellite switches quickly from the nominal three-axis control mode to the sun-pointing spin stabilized mode by power-off of the reaction wheel. Only the minimum set of onboard instruments keep power-on for power saving. The onboard processor works in the triple voting ROM mode. According to the five years' heritage of REIMEI operation, this safe-hold sequence has been triggered in orbit once or twice a year, when scientists try a risky observation plan for ambitious sciences that requires a large discharge from batteries.

3. Serious OBC Anomaly and Hardware UVC Detection. A non-maskable interrupt (NMI) of OBC such as a watch dog timer error and hardware detection of the batteries' under-voltage are a most serious satellite fault. In these two cases, the onboard computer switches from the triple voting configuration to the single processor ROM mode, and the attitude control switches to the sun-pointing spin stabilized mode. The former case (watch dog timer error) occurred once in June 21, 2006 at the SAA area that is indicated by the sign of \* in Fig. 15. It is reported that at that time a

solar storm was observed. This anomaly seems to be a very rare case such that during a reconfiguration process another SEU happens. The latter case (hardware detection of UVC) occurred once in July 21, 2010, when scientists tried a risky aurora observation for ambitious sciences above the south pole against the batteries surviving for five years.

In both cases REIMEI survived with a safe-hold mode. It took about a week for recovering operation from the safe-hold condition to the nominal observation mode. These operations show that REIMEI is a robust and reliable satellite.

### 7.3. Reliability of onboard software

Software of the onboard computer is developed fully in house by ISAS staff and students. Onboard software was verified at software tests, system tests on ground as well as at verifications prior to a satellite operation. Software consists of several tasks related to all the satellite functions. Therefore reliability of the software is significantly important.

Interfaces between these tasks are very complicated in case of an integrated control system such as ICU. We applied the CVS (Concurrent Versions System) software for management of software versions and found it very effective as follows: (1) integrated management of many source files (as many as 300 files), (2) integrations and collision managements of software which many people develop interactively, and (3) recording of source file versions at each ground test, such as a system test for onboard software.

### 7.4. Verifications of satellite and operation plan

Verifications and tests on ground are significantly useful to detect possible defects that could not be removed by careful designs and manufacturing processes.

In REIMEI a series of intensive ground tests were performed compared with other small satellites in Japan. Design defects and initial defects of hardware were detected through tests with various simulators and environmental tests with satellite functions being monitored.

Many of on-orbit malfunctions of small satellites may be related to their communication subsystem and power subsystem, which are fundamental functions of a satellite. Careful verification plans are mandatory even for inexpensive small satellites, although many small satellite projects are apt to pay less attention to them. After the careful verification tests described below, the REIMEI project were able to obtain sufficient confidence with the satellite functions.

For communication subsystem of REIMEI, the onboard components and the main ground station at Sagami-hara were newly developed. In addition to their individual verifications, compatibility tests with both systems being combined were carefully conducted. Also compatibility tests were performed at the Svalbard Satellite Station in Norway and Uchinoura 20 m station in Kyushu Japan with the proto model of onboard communication instruments.

For power subsystem, one must pay attention to their test configuration combining the power source (the solar paddles with light sources or an electrical solar simulator), the power control unit (the proto model or the flight model), the batteries, and the power loads (the satellite system or an electrical load). We conducted ground tests of power subsystem with the best configuration among them for each test purpose.

For attitude control subsystem, the verification tests consist of onboard component tests and subsystem tests. The component tests sometimes unveil their unexpected characteristics and give influences to satellite system. For example it was found in the solar simulator test that the baffle of the star tracker (STT) does not have enough optical attenuation capability, and a new sun shade was installed so that the baffle is not irradiated by sun light. The fiber optical gyroscopes (FOGs) are found to be more stabilized than expected in terms of their bias rate by the fine temperature control. This higher stability of FOGs contributes significantly to the fine attitude control accuracy [3,4].

For attitude control subsystem level, we conducted static open loop tests (SOLTs) and static close loop tests (SCLTs) without any motion simulators. The purpose of SOLTs is to verify the data interface between the component hardware and the ICU (the data handling unit). In the SCLTs we combined the ICU hardware, the flight software, the hardware simulators (circuits) of the attitude control components, and the dynamic simulator software, which simulate the satellite dynamics and the space environments (the sun, stars, and the geomagnetic field), in order to verify the end-to-end performance of the attitude control subsystem for typical control modes of the initial acquisition phase and the steady observation phase. The tests run in real time with the onboard computer. In addition to SCLTs, software simulation tests in PC were conducted to verify the control algorithm for wide range of parameters since software simulations can be performed in an accelerated speed.

For the system level with satellite being integrated, a limited number of typical satellite modes was tested in a configuration that is close to one in the orbit as much as possible. The typical satellite modes are the initial acquisition mode, the observation mode with three-axis control, and the safe-hold mode with sun-pointing spin stabilization. It is impossible to test all the functions of the satellite with being integrated. The SCLTs of the attitude control were not carried out with the satellite being integrated since we could not connect the hardware simulators of the attitude control components with the ICU. In the system level, we confirmed at least that the specific mode of each subsystem is triggered or initiated at the appropriate timing or condition by the ICU since details of the specific mode had already been verified at the subsystem test.

However, it was almost impossible that all the combinations of software tasks with various modes are verified prior to the launch since most of the functions of REIMEI satellite are processed by the onboard computer (ICU). Instead of the ground test, at the satellite operation phase, we verify the real combination of the operation modes prior to a real satellite operation as described in Section 6. We constructed a system for REIMEI operation where we can check whether the operation plan for the next pass is safe or not in terms of task combinations and parameters. With this operation system, verification for a specific combination of the operation modes is performed prior to a real satellite operation. No malfunction due to complexity of ICU occurred in orbit for five years because of the reliable satellite operation.

## 8. Conclusion

REIMEI is a small scientific satellite for aurora observation and advanced satellite technologies. It was launched into a nearly sun synchronous polar orbit on Aug. 23rd, 2005 (UTC) from Baikonur, Kazakhstan by Dnepr rocket. REIMEI satellite has been working satisfactorily on the orbit for five years at present as of January, 2011. The three-axis attitude control is achieved with accuracy of  $0.1^\circ$  ( $3\sigma$ ). REIMEI is performing the simultaneous observation of aurora images as well as particle measurements. REIMEI indicates that even a small satellite launched as a piggy-back can successfully perform the unique scientific mission purposes with high reliability.

## Acknowledgments

We deeply thank all of the REIMEI project team and the students of Saito Lab for their contribution. This paper is in the memory of Mr. T. Takahara.

## References

- [1] H. Saito, et al., REIMEI piggy-back satellite for aurora observation and technology demonstration, *Acta Astronaut.* 48 (5–12) (2001) 723–735.
- [2] H. Saito, Japan's small scientific satellite, "INDEX" (Reimei), in: H.H. Siegfried, W. Janson (Eds.), *Small Satellites: Past, Present, and*

- Future, American Institute of Aeronautics and Astronautics (AIAA), USA, 2010, pp. 449–485.
- [3] S. Sakai, et al., Design and evaluation of accurate attitude control system for small satellite REIMEI, *Inst. Electron. Inf. Commun. Eng. J88-B (1)* (2005) 69–78 in Japanese.
  - [4] S. Sakai, et al., Studies on magnetic attitude control system for the REIMEI Microsatellite, in: *Proceedings of the AIAA Guidance, Navigation, and Control Conference*, Keystone, Colorado, USA, 2006.
  - [5] S. Fukuda, et al., On-orbit performance of the reimei satellite with integrated computer system and introduction to its flexible operation, 2006-f-01, in: *Proceedings of the 25th International Symposium on Space Technology and Science (ISTS)*, 2006.
  - [6] Y. Sone, et al., The flight and ground test data of the lithium-ion secondary battery of 'REIMEI', 2006-f-04, in: *Proceedings of the 25th ISTS*, 2006.
  - [7] H. Saito, et al., Development and on-orbit results of solar concentrated paddles with thin film reflector, 2006-f-03, in: *Proceedings of the 25th ISTS*, 2006.
  - [8] N. Okuizumi, et al., Wrinkling and reflection characteristics of membrane solar reflectors of REIMEI spacecraft, 2006-c-14, in: *Proceedings of the 25th ISTS*, 2006.
  - [9] Y. Nakamura, et al., In orbit test result of smart radiation device, 2006-c-20, in: *Proceedings of the 25th ISTS*, 2006.
  - [10] H. Saito, et al., Tiny GPS receiver for space application, *Inst. Electron. Inf. Commun. Eng. J88-B (1)* (2005) 79–89 in Japanese.
  - [11] H. Saito et al., Development and on-orbit results of miniature space GPS receiver by means of automobile-navigation technology, 2006-f-02, in: *Proceedings of the 25th ISTS*, 2006.
  - [12] <<http://spacelink.biz/>>.
  - [13] J.M. Bodeu, Root cause of the BSS 702 concentrator array anomaly, *Space Power Workshop*, April, 2003.
  - [14] T. Sakanoi, S. Okano, Y. Obuchi, T. Kobayashi, M. Ejiri, K. Asamura, M. Hirahara, Development of the multi-spectral auroral camera onboard the index satellite, *Adv. Space Res.* 32 (3) (2003) 379–384.
  - [15] K. Asamura, D. Tsujita, H. Tanaka, Y. Saito, T. Mukai, M. Hirahara, Auroral particle instrument onboard the INDEX satellite, *Adv. Space Res.* 32 (3) (2003) 375–378.
  - [16] H. Saito, et al., An overview and lessons learned of small scientific satellite "INDEX" (REIMEI), IAC-07-B4.4.05, in: *Proceedings of the 58th International Astronautical Congress*, 2007.
  - [17] K. Asamura, C.C. Chaston, Y. Itoh, M. Fujimoto, T. Sakanoi, Y. Ebihara, A. Yamazaki, M. Hirahara, K. Seki, Y. Kasaba, M. Okada, Sheared flows and small-scale Alfvén wave generation in the auroral acceleration region, *Geophys. Res. Lett.*, 36, L05105, 10.1029/2008GL036803, 2009.
  - [18] C.C. Chaston, K. Seki, T. Sakanoi, K. Asamura, M. Hirahara, The Motion of Aurorae, *Geophys. Res. Lett.* (2010).
  - [19] D. Bearden, Small-Satellite Costs, Crosslink (Winter, 2001); available at <<http://www.aero.org/publications/crosslink/winter2001/04.html>>.
  - [20] M. Tafazoli, A study of on-orbit spacecraft failures, in: *Proceedings of the Paper D1.5.02*, presented at the 58th International Astronautical Congress, Sept. 2007.